



Effect of annealing temperature on structure, magnetic properties and optical characteristics in $\text{Zn}_{0.97}\text{Cr}_{0.03}\text{O}$ nanoparticles

Yang Liu^{a,b}, Jinghai Yang^{b,*}, Qingfeng Guan^{a,*}, Lili Yang^b, Huilian Liu^b, Yongjun Zhang^b, Yaxin Wang^b, Dandan Wang^c, Jihui Lang^{a,b}, Yanting Yang^b, Lianhua Fei^b, Maobin Wei^b

^aSchool of Material Science and Engineering, Jiangsu University, Zhenjiang, 212013, PR China

^bCollege of Physics, Jilin Normal University, Siping, 136000, PR China

^cKey Laboratory of Excited State Processes, Changchun Institute of Optics, Fine Mechanics and Physics Chinese Academy of Sciences, Changchun, 130033, PR China

ARTICLE INFO

Article history:

Received 27 June 2009

Received in revised form 1 December 2009

Accepted 23 December 2009

Available online 4 January 2010

Keywords:

Cr-doped ZnO

Ferromagnetism

Photoluminescence

Sol–gel

ABSTRACT

The Cr-doped zinc oxide ($\text{Zn}_{0.97}\text{Cr}_{0.03}\text{O}$) nanoparticles were successfully synthesized by sol–gel method. The relationship between the annealing temperature (400 °C, 450 °C, 500 °C and 600 °C) and the structure, magnetic properties and the optical characteristics of the produced samples was studied. The results indicate that Cr (Cr^{3+}) ions at least partially substitute Zn (Zn^{2+}) ions successfully. Energy dispersive spectroscopy (EDS) measurement showed the existence of Cr ion in the Cr-doped ZnO. The samples sintered in air under the temperature of 450 °C had single wurtzite ZnO structure with prominent ferromagnetism at room temperature, while in samples sintered in air at 500 °C, a second phase-ZnCr₂O₄ was observed and the samples were not saturated in the field of 10000 Oe. This indicated that they were mixtures of ferromagnetic materials and paramagnetic materials. Compared with the results of the photoluminescence (PL) spectra, it was reasonably concluded that the ferromagnetism observed in the studied samples was originated from the doping of Cr in the lattice of ZnO crystallites.

© 2009 Elsevier B.V. All rights reserved.

1. Introduction

Semiconductors doped with transition metal elements or rare earths, referred to as diluted magnetic semiconductors (DMSS), have potential applications in spintronics devices [1]. ZnO-based DMS may also become a highly multifunctional material with coexisting magnetic, semiconducting, electromechanical and optical properties, and it has been studied extensively in recent years [2–4].

Theoretical works have predicted that high-temperature ferromagnetism (FM) should exist in the TM-doped ZnO systems [5], but the experimental results are quite contradictory. Although room temperature FM has been found [6], there are still some reports showing no sign of FM, or suggesting the presence of secondary phase as the origin of FM [7,8]. Until now, there is still no definite agreement on the nature of the FM in DMSS. Various groups have performed magnetic studies on Cr-doped ZnO samples [9,10]. Cr is an important transition metal element with closer ionic (Cr^{3+}) radius parameter to that of Zn^{2+} , which means that Cr^{3+} can easily penetrate into the ZnO crystal lattice or substitute the position of Zn^{2+} in the crystal ZnO [11]. However,

compared with the widely studied Co- or Mn-doped ZnO [12,13] systems, both theoretical and experimental researches on the Cr-doped ZnO are still limited. Therefore, the magnetic properties of Cr-doped ZnO are far from being clear and more detailed and probing investigations are necessary to reveal the nature of this material.

In the present work, we report that we dope Cr into ZnO with varying annealing temperatures by decomposing citrate technique and achieve room temperature ferromagnetism. We mainly study the effects of annealing temperature on PL property and ferromagnetism in $\text{Zn}_{0.97}\text{Cr}_{0.03}\text{O}$ nanoparticles. The origin of the ferromagnetism in $\text{Zn}_{0.97}\text{Cr}_{0.03}\text{O}$ nanoparticles is discussed.

2. Experimental

All chemical reagents in our experiment were of analytical grade purity. The initial materials included $\text{Zn}(\text{NO}_3)_2 \cdot 6\text{H}_2\text{O}$, $\text{Cr}(\text{NO}_3)_3 \cdot 9\text{H}_2\text{O}$ and $\text{C}_6\text{H}_8\text{O}_7 \cdot \text{H}_2\text{O}$. The appropriate stoichiometric proportions of $\text{Zn}(\text{NO}_3)_2 \cdot 6\text{H}_2\text{O}$, $\text{Cr}(\text{NO}_3)_3 \cdot 9\text{H}_2\text{O}$ and $\text{C}_6\text{H}_8\text{O}_7 \cdot \text{H}_2\text{O}$ were weighed (Zn: Cr = 0.97:0.03, in mol) and their solutions were mixed. The mixture was homogenized with stirring for 2 h to form a sol. The mixture subsequently polymerized to form a gel at 80 °C. The gel was prepyrolyzed to become an amorphous composite precursor at 130 °C. In air atmosphere, the precursors were heated up to 400 °C, 450 °C, 500 °C and 600 °C, respectively. Then they

* Corresponding authors. Tel.: +86 434 3294566; fax: +86 434 3294566.

E-mail addresses: jhyang1@jlnu.edu.cn (J. Yang), guanqf@ujls.edu.cn (Q. Guan).

were kept at these temperatures for 10 h. After being cooled to room temperature, the samples were obtained.

The structural characterization of $\text{Zn}_{0.97}\text{Cr}_{0.03}\text{O}$ was performed by X-ray diffraction (XRD) on D/max-2500 copper rotating-anode X-ray diffractometer with $\text{Cu K}\alpha$ radiation (40 kV, 200 mA). The size distribution and interplanar distance were investigated by the transmission electron microscope (TEM) (200 keV, JEM-2100HR, Japan). The magnetic hysteresis loops of $\text{Zn}_{0.97}\text{Cr}_{0.03}\text{O}$ were measured by a Lake Shore 7407 vibrating sample magnetometer (VSM). The valence state of the Cr element was analyzed by X-ray photoelectron spectroscopy (XPS) (VG ESCALAB Mark II). PL measurement was performed on an HR800 Labram Infinity Spectrophotometer, excited by a continuous He–Cd laser at a wavelength of 325 nm and a power of 50 mW.

3. Results and discussion

Fig. 1 shows the XRD patterns of the samples annealed at 400 °C, 450 °C, 500 °C and 600 °C. The apparent reduction of FWHM (full width at half maximum) and increase of intensity show the continuous growing-up of the particle size with the improvement of the synthesis temperature. The average particle size of the samples obtained at 400 °C, 450 °C, 500 °C and 600 °C are 11.1 nm, 12.5 nm, 18.9 nm and 45.2 nm, respectively, by Debye–Scherrer formula. When the temperature is 500 °C, the diffraction peaks at

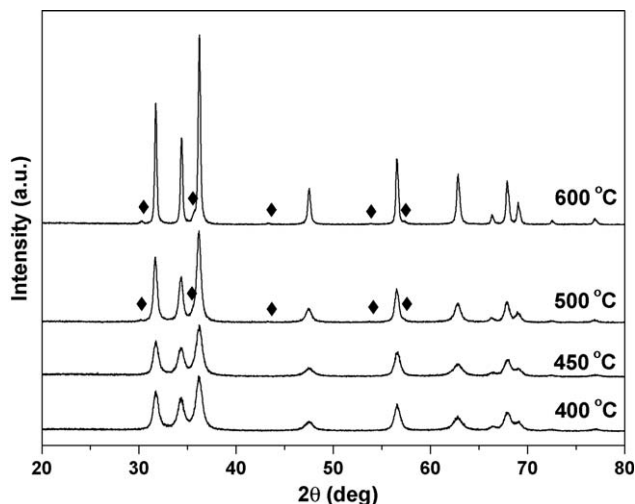


Fig. 1. XRD patterns for the samples annealed at different temperatures. ◆ indicates the peaks of the impurity phase of ZnCr_2O_4 .

$2\theta = 30.1^\circ, 35.4^\circ, 43.5^\circ, 53.7^\circ$ and 57.4° (attributed to ZnCr_2O_4) appear, it indicates that sintering temperature should be below 450 °C so as to obtain single-phase $\text{Zn}_{0.97}\text{Cr}_{0.03}\text{O}$. The reason is that when the sintering temperature is too high, Cr ions diffused in ZnO

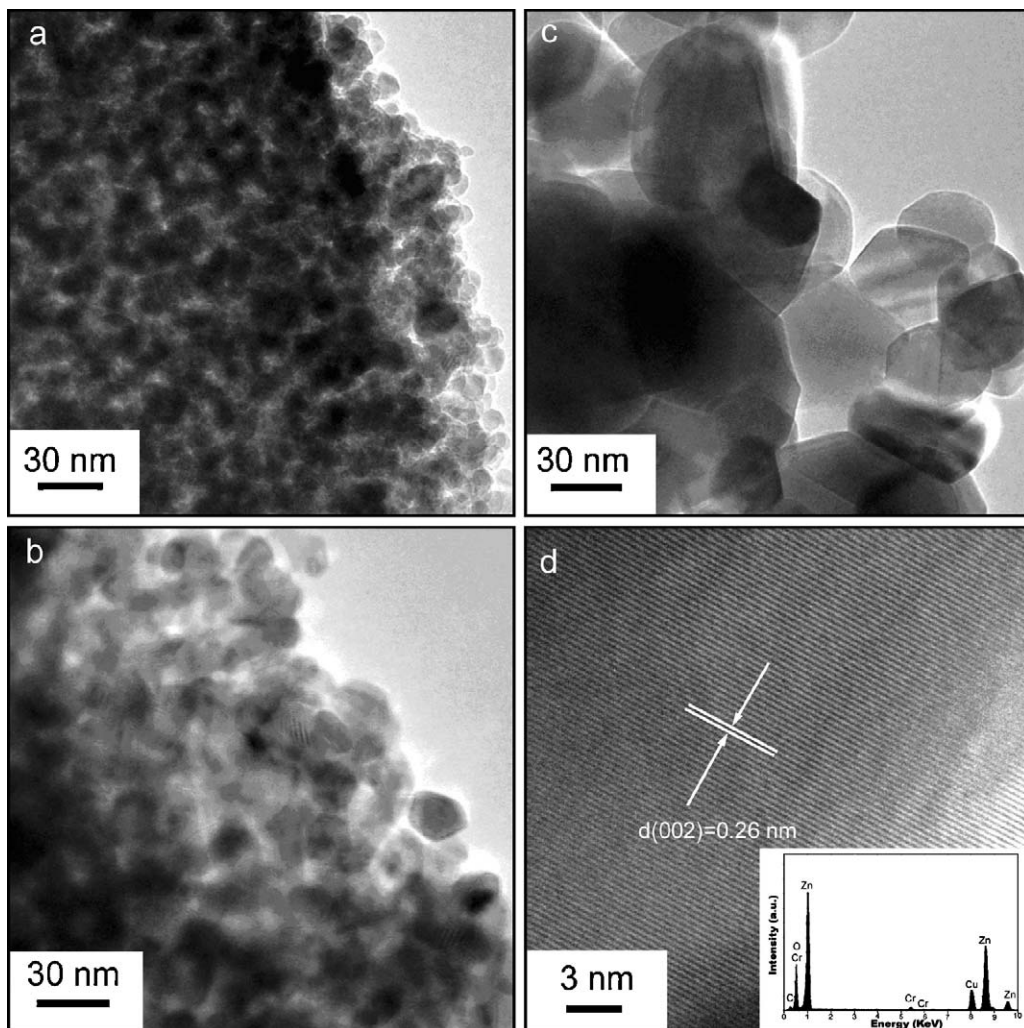


Fig. 2. TEM images of $\text{Zn}_{0.97}\text{Cr}_{0.03}\text{O}$ nanoparticles annealed at 400 °C (a), 500 °C (b) and 600 °C (c); HRTEM images of $\text{Zn}_{0.97}\text{Cr}_{0.03}\text{O}$ nanoparticles annealed at 400 °C (d); the inset figure is the EDS spectrum.

crystal are separated from ZnO, and generate new phase with the ambient Zn and O ions, which leads to the appearance of ZnCr_2O_4 .

Figs. 2(a)–(c) shows the TEM image of the samples annealed at 400 °C, 500 °C and 600 °C. It can be seen that the sample is spherical shape and it has a narrow size distribution. The average particle size is about 10 nm, 20 nm and 46 nm for the sample annealed at 400 °C, 500 °C and 600 °C respectively, which is in agreement with the results of the XRD. Fig. 2(d) shows the high-resolution transmission electron microscopy (HRTEM) image of the samples annealed at 400 °C. It can be clearly observed that the interplanar distance of fringes is 0.26 nm matching the (0 0 2) planes of wurtzite ZnO. This result indicates that Cr ions are likely to be incorporated into the crystal lattice of ZnO. We examined the amount of the Cr-doping by EDS. The inset of Fig. 2(d) shows the EDS for a single $\text{Zn}_{0.97}\text{Cr}_{0.03}\text{O}$ nanoparticle annealed at 400 °C. It can be seen that an oxygen peak is at about 0.53 keV, Zn peaks are at about 1.02 keV, 8.68 keV and 9.62 keV and Cr peaks are at about 0.54 keV, 5.38 keV and 5.82 keV. The Cu peak at about 8.05 keV and the C peak at about 0.30 keV come from copper grid [14]. The quantitative EDS analysis reveals that the molar ratio of Cr is about 3 at% in each Cr-doped ZnO nanoparticle. The statistic analysis of EDS measurements over many of the $\text{Zn}_{0.97}\text{Cr}_{0.03}\text{O}$ nanoparticles shows that the variation of the Cr content is rather small. It demonstrates that the Cr dopant is uniform throughout the sample. From the above XRD results, the sample annealed at 400 °C has no diffraction peaks of Cr or Cr compounds elementary substance, which further testifies the probability that Cr is incorporated into ZnO.

The high-resolution scans of the XPS spectra of Zn 2p, O 1s and Cr 2p are shown in Fig. 3 for the $\text{Zn}_{0.97}\text{Cr}_{0.03}\text{O}$ nanoparticles annealed at 400 °C. The peaks located at 1020 eV and 1043 eV correspond to that of Zn $2p_{3/2}$ and Zn $2p_{1/2}$, respectively. The O 1s spectrum exhibits only a single peak at 530.4 eV, which can be fitted by a Gaussian line profile. Brundle et al. reported that the peak was associated with photoemission in O^{2-} ions with valence state comparable to that of oxygen found in a bulk ZnO crystal. Moreover, the core level binding energy observed for Cr $2p_{3/2}$ peak locates in the vicinity of 576.6 eV. Obviously, that is clearly different from 574.2 eV of Cr metal and 576.0 eV of Cr^{2+} . This peak can be indexed to Cr^{3+} ions as they match well with the reported binding energy of Cr^{3+} states [11]. Generally speaking, if Cr is present in the substitutional site in a defect-free ZnO crystal, the valence state of Cr will be +2. However, the result of XPS confirms the presence of uncoupled Cr^{3+} within the sample. It suggests that Cr dopants may be incorporated into the ZnO lattice as Cr^{3+} ions instead of Cr^{2+} ions.

Fig. 4 shows the hysteresis loops of $\text{Zn}_{0.97}\text{Cr}_{0.03}\text{O}$ nanoparticles measured at room temperature for the samples annealed at 400 °C, 450 °C, 500 °C and 600 °C. The $\text{Zn}_{0.97}\text{Cr}_{0.03}\text{O}$ nanoparticles annealed at 400 °C show clear magnetic hysteresis loops, which indicate that they have good ferromagnetic property at room temperature. Similar results are found for the samples annealed at 450 °C. From Fig. 4, we can find that when the sintering temperature increases from 400 °C to 450 °C, magnetization of the sample drops sharply. That is because when the ZnO are heated, they tend to lose oxygen [15]. Therefore, the defect-induced FM would be increased. Similar decreasing trend of magnetization is also observed in other $\text{Zn}_{1-x}\text{Cr}_x\text{O}$ powders and films [16].

It is worth noting that the samples are not saturated in the field of 10,000 Oe when the temperature reaches 500 °C or 600 °C. That indicates that they were mixtures of ferromagnetic materials and paramagnetic materials. According to the XRD results, Cr ions are separated from ZnO, which leads to the appearance of the second phase- ZnCr_2O_4 . ZnCr_2O_4 shows paramagnetic property at the room temperature (the Neel temperature is 11 K) [17]. In addition, the antiferromagnetic coupling between Cr^{3+} – Cr^{3+} may contribute to

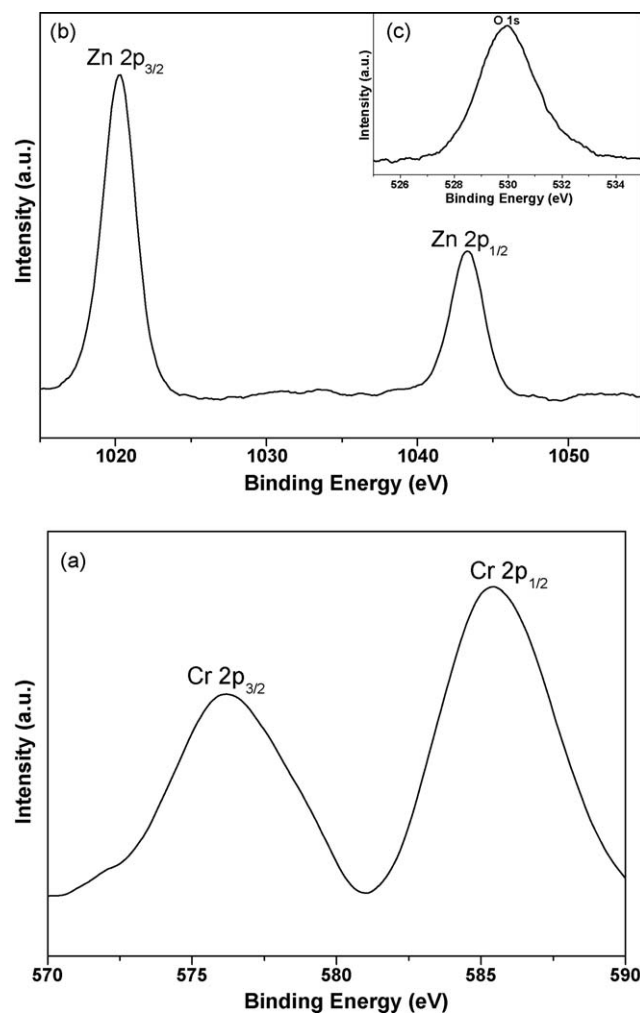


Fig. 3. XPS spectrum of the $\text{Zn}_{0.97}\text{Cr}_{0.03}\text{O}$ nanoparticles annealed at 400 °C. (a)–(c) Showed the high-resolution scans of Cr 2p, Zn 2p and O 1s.

this phenomenon. That further proves that the $\text{Zn}_{0.97}\text{Cr}_{0.03}\text{O}$ nanoparticles obtained below 450 °C is a single-phase.

The room temperature PL spectra for the $\text{Zn}_{0.97}\text{Cr}_{0.03}\text{O}$ nanoparticles sintered at 400 °C, 450 °C and 500 °C are shown in Fig. 5, respectively. A strong ultraviolet (UV) emission peak around

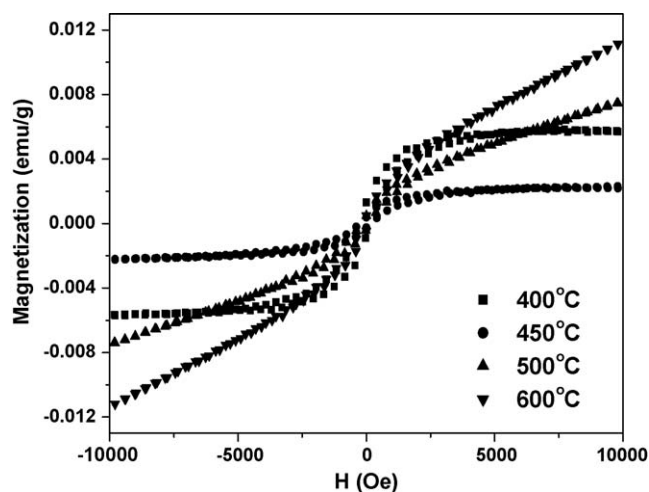


Fig. 4. Magnetic hysteresis (M–H) loops of $\text{Zn}_{0.97}\text{Cr}_{0.03}\text{O}$ annealed at 400 °C, 450 °C, 500 °C and 600 °C under 10 KOe.

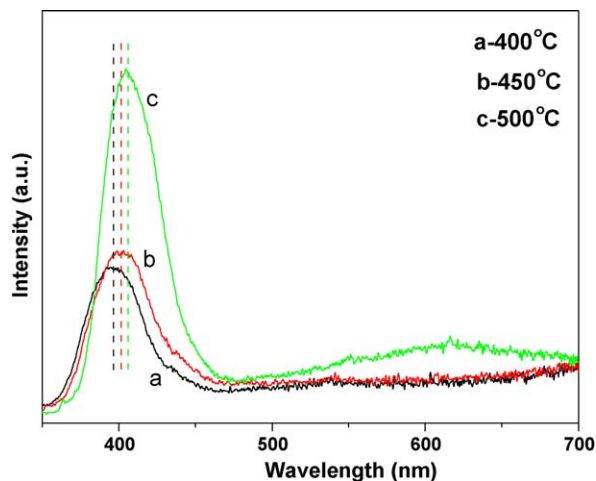


Fig. 5. PL spectra of $\text{Zn}_{0.97}\text{Cr}_{0.03}\text{O}$ nanoparticles annealed at 400 °C, 450 °C and 500 °C.

390–400 nm is observed. As the annealing temperature increases, the UV peak red-shifts and the intensity also increases. The peak positions of PL spectra are significantly dependent on the size of the ZnO crystalline due to the quantum-confinement effect, which will induce gap enhancement [18]. The size of ZnO nanoparticles decreases from 46 nm to 10 nm in our case. So the red-shift for UV emission may be related to the quantum-confinement effect of the ZnO nanocrystal. Meanwhile, the enhancement of the UV intensity with the increase of the annealing temperature is mainly due to the improvement of crystalline, which is coincided with the XRD characterization results.

An unusual but interesting feature of our PL spectra is that the deep level emission (DLE) is very weak for the sample grown under 400 °C and 450 °C. This result is in good agreement with the report of Issei Satoh et al. [19], in which they had mentioned that the Cr-doping in ZnO had significant effect on the quenching of DLE of ZnO. DLE has been attributed to the oxygen vacancy (V_{O}) and the zinc vacancy (V_{Zn}) [20,21]. Therefore, the results show that the Cr-doping decreases the quantity of the defect.

The origin of FM in TM-doped ZnO samples is still undetermined. A number of studies indicate that the FM in TM-doped ZnO may come from the precipitation of magnetic clusters or from the secondary magnetic phases [22]. But the results of XRD, XPS and VSM exclude the possibility of the existence of the secondary phases in our samples. Double exchange mechanism between d states of TM elements is another possible candidate to induce ferromagnetism in magnetic oxide [23]. However, the low doping concentration of 3% and single valence state (+3) of the doped chemical elements have been observed to exclude the double exchange mechanism. In addition, several groups have found that the point defects play crucial roles in the FM of ZnO-based DMs [24,25]. Zhuge et al. [26] have found that the magnetization in their Cr-doped ZnO films is correlated to the V_{Zn} . Hong et al. [27] ascribed the FM in Cr-doped ZnO films to the V_{O} . But the results of PL eliminate this probability. In summary, we conclude that the ferromagnetism of the $\text{Zn}_{0.97}\text{Cr}_{0.03}\text{O}$ nanoparticles in this study is an intrinsic property of the Cr-doped ZnO. It is noted that the magnetic properties of the Cr-doped ZnO are sensitive to the preparation method. More detailed work is essential in order to understand the magnetic behaviors of these materials.

4. Conclusions

In this paper, the $\text{Zn}_{0.97}\text{Cr}_{0.03}\text{O}$ nanoparticles were synthesized by sol–gel method. The relationship between the annealing

temperature and structure, the magnetic properties and optical characteristics of the samples was studied. Different measuring equipments were used to characterize the structure of the $\text{Zn}_{0.97}\text{Cr}_{0.03}\text{O}$ nanoparticles annealed below 450 °C. At last, we verified in success that Cr ions probably took the place of Zn ions as +3 valence state in ZnO lattice. The samples sintered below 450 °C have good ferromagnetic property at room temperature. While in samples sintered in air at 500 °C, the samples were mixtures of ferromagnetic materials and paramagnetic materials due to the appearance of ZnCr_2O_4 . Comparing with the analysis of the PL spectrum, we think the ferromagnetism observed in the studied samples was an intrinsic property of the Cr-doped ZnO.

Acknowledgement

This work is supported by the National Programs for High Technology Research and Development of China (863) (Item Nos. 2009AA03E303 and 2007AA03Z400448), the National Natural Science Foundation of China (Grant Nos. 60778040 and 60878039), the National Youth Program Foundation of China (Grant No. 10804036), Program for the development of Science and Technology of Jilin province (Item Nos. 20082112 and 20080514), the Eleventh Five-Year Program for Science and Technology of Education Department of Jilin Province (Item Nos. 20070149 and 20080154).

References

- [1] S.A. Wolf, D.D. Awschalom, R.A. Buhrman, J.M. Daughton, S. von Molnar, M.L. Roukes, A.Y. Chtchelkanova, D.M. Treger, *Science* 94 (2001) 1488.
- [2] Q. Wang, Q. Sun, P. Jena, Y. Kawazoe, *Appl. Phys. Lett.* 87 (2005) 162509.
- [3] S.B. Ogale, R.J. Choudhary, J.P. Buban, S.E. Lofland, S.R. Shinde, S.N. Kale, V.N. Kulkarni, J. Higgins, C. Lanci, J.R. Simpson, N.D. Browning, S. Das Sarma, H.D. Drew, R.L. Greene, T. Venkatesan, *Phys. Rev. Lett.* 90 (2003) 077205.
- [4] N. Tahir, S.T. Hussain, M. Usman, S.K. Hasanain, A. Mumtaz, *Appl. Surf. Sci.* (2008), doi:10.1016/j.apsusc.2009.06.003.
- [5] T. Dietl, H. Ohno, F. Matsukura, J. Cibert, D. Ferrand, *Science* 287 (2000) 1019.
- [6] K. Bradley, Roberts, B. Alexandre, Pakhomov, M. Kannan, Krishnan, *J. Appl. Phys.* 103 (2008) 133.
- [7] K. Ueda, H. Tabata, T. Kawai, *Appl. Phys. Lett.* 79 (2001) 988.
- [8] Z. Jin, T. Fukumura, M. Kawasaki, K. Ando, H. Saito, T. Sekiguchi, Y.Z. Yoo, M. Murakami, Y. Matsumoto, T. Hasegawa, H. Koinuma, *Appl. Phys. Lett.* 78 (2001) 3824.
- [9] L. Schneider, S.V. Zaitsev, W. Jin, A. Kompch, M. Winterer, M. Acet, G. Bacher, *Nanotechnology* 20 (2009) 135604.
- [10] L.Y. Li, H. Liu, X.G. Luo, X. Zhang, W.H. Wang, Y.H. Cheng, Q.G. Song, *Solid State Commun.* 146 (2008) 420.
- [11] B.Q. Wang, J. Iqbal, X.D. Shan, G.W. Huang, H.G. Fu, R.H. Yu, D.P. Yu, *Mater. Chem. Phys.* 113 (2009) 103.
- [12] J.H. Yang, L.Y. Zhao, Y.J. Zhang, Y.X. Wang, H.L. Liu, *J. Alloys Compd.* 473 (2009) 543.
- [13] D. Paul Joseph, G. Senthil Kumar, C. Venkateswaran, *Mater. Lett.* 59 (2005) 2720.
- [14] L.Q. Liu, B. Xiang, Y. Zhang, D.P. Yu, *Appl. Phys. Lett.* 88 (2006) 063104.
- [15] L.V. Azaroff, *Introduction to Solids*, McGraw-Hill, 1960., p. 371.
- [16] H. Liu, X. Zhang, L.Y. Li, Y.X. Wang, K.H. Gao, Z.Q. Li, R.K. Zheng, S.P. Ringer, B. Zhang, X.X. Zhang, *Appl. Phys. Lett.* 91 (2007) 072511.
- [17] S.H. Lee, C. Broholm, T.H. Kim, W. Ratcliff, S.W. Cheong, *Phys. Rev. Lett.* 84 (2000) 3718.
- [18] N. Yang, H.B. Yang, Y.Q. Qu, Y.Z. Fan, L.X. Chang, H.Y. Zhu, M.H. Li, G.T. Zou, *Mater. Res. Bull.* 41 (2006) 2154.
- [19] Issei Satoh, Takeshi Kobayashi, *Appl. Surf. Sci.* 216 (2003) 603.
- [20] Q.X. Zhao, P. Klason, M. Willander, H.M. Zhong, W. Lu, J.H. Yang, *Appl. Phys. Lett.* 87 (2005) 211912.
- [21] T. Moe Børseth, B.G. Svensson, A.Yu. Kuznetsov, P. Klason, Q.X. Zhao, M. Willander, *Appl. Phys. Lett.* 89 (2006) 262112.
- [22] Ramachandran, Ashutosh Tiwari, J. Narayan, *Appl. Phys. Lett.* 84 (2004) 5255.
- [23] P.M. Krstajic, F.M. Peeters, V.A. Ivanov, V. Fleurov, K. Kikoin, *Phys. Rev. B* 70 (2004) 195215.
- [24] G.Z. Xing, J.B. Yi, J.G. Tao, T. Liu, L.M. Wong, Z. Zhang, G.P. Li, S.J. Wang, J. Ding, T.C. Sum, C.H.A. Huan, T. Wu, *Adv. Mater.* 20 (2008) 3521.
- [25] G.Z. Xing, J.B. Yi, D.D. Wang, L. Liao, T. Yu, Z.X. Shen, C.H.A. Huan, T.C. Sum, J. Ding, T. Wu, *Phys. Rev. B* 79 (2009) 174406.
- [26] L.J. Zhuge, X.M. Wu, Z.F. Wu, X.M. Chen, Y.D. Meng, *Scripta Mater.* 60 (2009) 214.
- [27] N.H. Hong, J. Sakai, N.T. Huong, N. Poirer, A. Ruyter, *Phys. Rev. B* 72 (2005) 045336.